J. Fluid Mech. (1966), *vol.* 24, *part* 2, *pp.* 209–223
Printed in Great Britain

Pressure distribution and mass injection effects in the transitional separated flow over a spiked body at supersonic speed

By MANSOP HAHN
Department of Aeronautical Engineering, Seoul National University, Korea

(Received 30 July 1964 and in revised form 23 February 1965)

Pressure distribution and the effect of air injection in the separated flow over a spiked-hemisphere were investigated at a Mach number of 3·3, and Reynolds number around the transitional value. Pressure distribution along the spike as well as over the body was measured in the absence of injection. Air was injected into the separated flow at the spike tip and base and reattachment region through one or more orifices drilled normal to the surface, and the resulting flow patterns were observed using the schlieren technique. The results show that (i) the pressure variation along the spike is similar to a two-dimensional separated flow in the transition régime; and (ii) the mass injection at the spike tip has a strong destabilizing effect regardless of injection rate, while the injection from spike base and reattachment region can be either slightly stabilizing or destabilizing depending on the flow condition.

1. Introduction

The front separated flow produced by a spiked-body has been studied as a means to reduce drag and heat-transfer rate by various investigators (e.g. Bogdonoff & Vas 1959; Wood 1962). Among these investigators, Wood conceived of injecting the cool gas into the separated flow with intent to improve the undesirable heat-transfer characteristics of the separated flow. In order to investigate the effect of mass injection on heat-transfer characteristics of the spiked-body, however, one requires knowledge of the coupling between the two flow configurations, i.e. separation and injection. The purpose of the present investigation is to study this coupling, i.e. to examine the effect of air injection at three different points in the separated flow on the flow pattern produced by a spiked-hemisphere, in the transitional Reynolds-number régime. Air was injected from (i) tip of the spike, (ii) base of the spike, and (iii) region of reattachment of separated boundary. The stability of the flow, transition characteristics and the deformation of the separated boundary are observed by schlieren technique. In order to investigate the basic characteristics of the separated boundary on the spike, the pressure distribution was measured along the spike in the absence of injection and related to the transition characteristics. In the earlier part of the present investigation, some of the tests carried out by Crawford (1959) were reproduced to confirm that the transition characteristics in the absence of injection at $M = 3{\cdot}3$, at which the present work is carried out, are essentially the

same as those for $M = 6{\cdot}8$, except for a shift in corresponding Reynolds number, thereby showing the feasibility of extending the conclusions of the present work to higher Mach numbers. The latter part of the paper describes and discusses the main results of the pressure measurement and mass injection. As supporting evidence, the flow is also perturbed by a trip near the spike tip to show that the tip injection is equivalent to increasing the the initial turbulence.

2. Experimental apparatus and models

The experiment was conducted in the Seoul National University 2×2 in. supersonic wind tunnel (Hahn 1964*a*). The experiment was carried out at the Mach number of $3{\cdot}26 \pm 1\%$. The tunnel stagnation pressure was varied from 14·7 to 230 psia, and the test Reynolds number, based on body diameter and free-stream conditions, varied from $0{\cdot}12 \times 10^6$ to $1{\cdot}91 \times 10^6$.

A photograph and sketch of the models used are shown in figures 1 (plate 1) and 2, respectively. All models were made of brass and were 0·709 in. in diameter. A stainless steel tube of 0·047 in. O.D. and 0·032 in. I.D., with the shoulder at the tip faired as shown in figure 2, was used as the spike. For some of the tests a boundary-layer trip of 0·0039 in. diameter wire was placed around the spike shoulder (figure 3 (*b*), plate 2). Static pressure along the spike was taken by drilling a hole of 0·018 in. diameter through the wall of the spike-tube. The model for

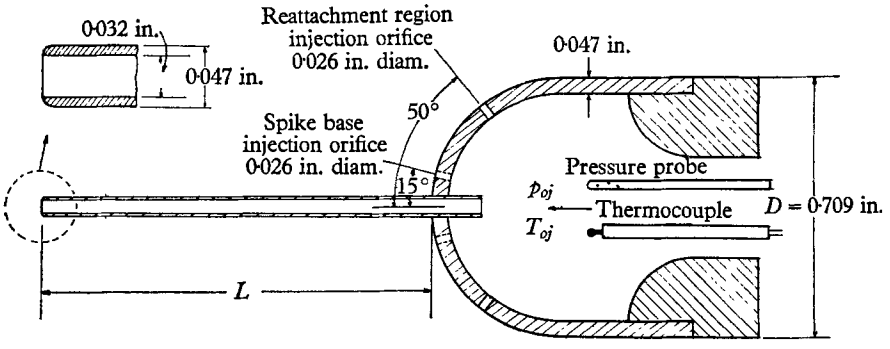

FIGURE 2. Cross-sectional sketch of injection model.

injection from spike base had 8 holes of 0·026 in. diameter equally spaced at 15° polar-angle away from the stagnation point, as shown in figures 1 and 2. The model for injection from reattachment region had 32 holes of 0·026 in. diameter at 50° from the stagnation point. All the injection holes were drilled normal to the body surface and no effort was made to contour the ejecting lip. For the flow-rate measurement a pressure probe and thermocouple were placed in the plenum chamber of the models (figure 2).

A single-pass micro-schlieren system (Hahn 1964*b*; Bradfield & Shepard 1959) was used for flow observation. The micro-schlieren field of view did not cover the entire flow field, and therefore two or three separate pictures were taken for each test to observe the whole field. A B-H 6 mercury vapour lamp was used as

the instantaneous light source which lasted a few microseconds. Several pictures were taken at 1 or 2 sec interval for each test. More than 600 pictures in all were used to deduce the following arguments.

3. Results for flow without injection

3.1. *Nature of the separated flow*

Typical pictures of the flow without injection are shown in the schlieren photographs of figures 3 (*a*) to (*d*) (plate 2) and are sketched in figure 4. The results for the spike with $L/D = 1{\cdot}5$ show that the separation starts from the spike tip for

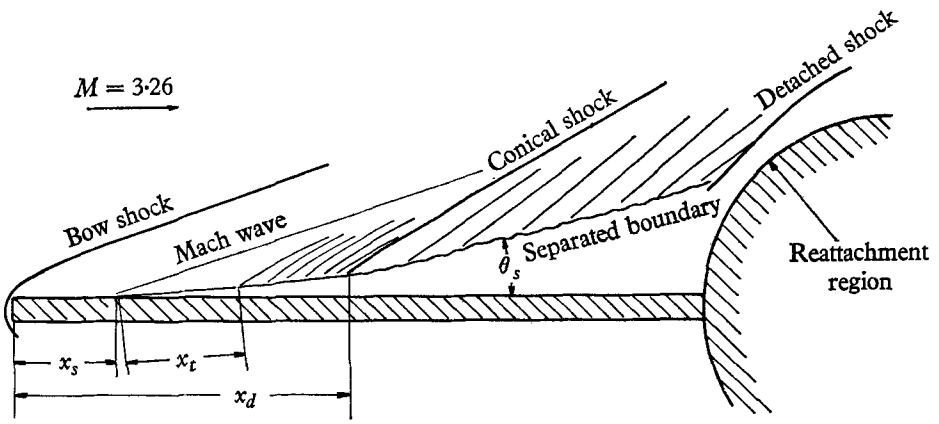

FIGURE 4. Sketch of the observed flow field without injection.

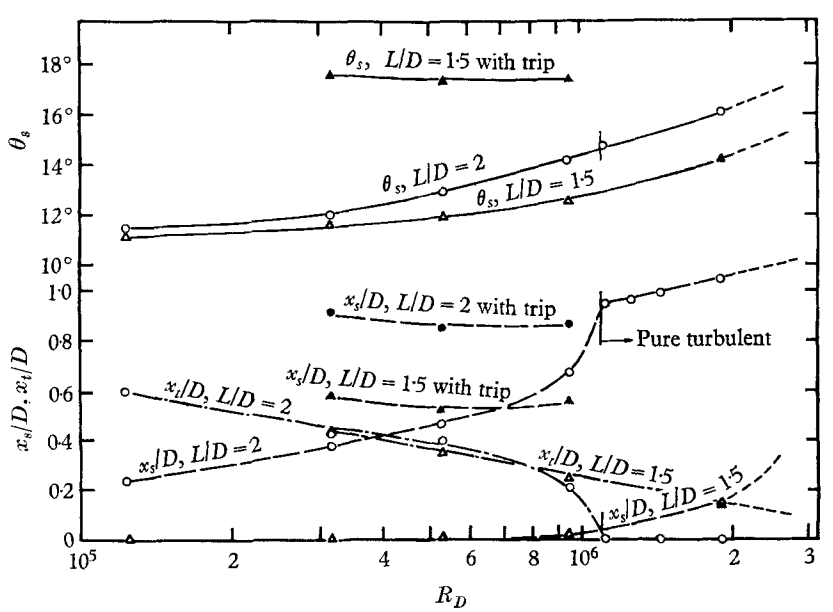

FIGURE 5. Summary of separation point, separated boundary length to transition, and separation angle, for different Reynolds numbers.

Reynolds number R_D below $0{\cdot}95 \times 10^6$, where R_D is the Reynolds number based on model diameter and free-stream conditions, but some finite distance behind the tip for Reynolds number above $1{\cdot}91 \times 10^6$. Here L and D are the spike length and model diameter, respectively. For the spike with $L/D = 2$, the flow separation starts always at finite distance behind the tip (figures 3(*c*) and (*d*), plate 2). For comparison, the same flow was perturbed by placing a boundary-layer trip near the tip of the spike (figure 3(*b*)). For both $L/D = 1{\cdot}5$ and 2, the tripping caused a rearward shifting of the separation point for R_D below $0{\cdot}95 \times 10^6$ (figure 5). This fact, together with the following pressure measurement (§3.2), confirmed that the starting condition of separation without a trip is laminar for R_D below $0{\cdot}95 \times 10^6$ for both spike lengths. For the determination of the separation point, the onset of separation was identified by the origin of the Mach wave emanating from the spike surface (figure 4). For $L/D = 2$, a pure turbulent separation was observed for Reynolds numbers above $1{\cdot}09 \times 10^6$.

The data for the spike with $L/D = 2$ show that the laminar separation point moves rearward with an increase in Reynolds number, as shown in figures 5 and 7, where scatter is indicated by the length of the bar. The rearward movement of the separation point with increasing Reynolds number was confirmed by the pressure measurements (§3.2).

As Reynolds number increases, the extent of the laminar separated boundary, x_l (figure 4), decreases (see figures 5 to 7). The transition point of the separated boundary is seen from the photographs (figures 3(*a*) and (*c*), plate 2) as the starting point of the wavy boundary, where many Mach waves are generated (see e.g. Chapman, Kuehn & Larson 1957). The unsteadiness of the wavy boundary was confirmed by comparing several pictures taken at different instances in the same run. The average transition point, together with an approximate transition region, is indicated in figures 6 and 7. For the lowest R_D tested, the flow was found to be unsteady in the rear part of the separated boundary, and the detached shock wave generated in front of the reattachment region oscillated with a small amplitude. These facts confirmed that a transitional separation takes place even for the lowest Reynolds number tested. This result agrees with that of Stalder & Nielsen (1954), who obtained a transitional separation at

$$R_D = 0{\cdot}155 \times 10^6 \quad \text{for} \quad M = 2{\cdot}67,$$

and also supports the result of Crawford (1959) and Chapman *et al.* (1957). Pure laminar separation was obtained by Crawford at $R_D = 0{\cdot}13 \times 10^6$ and $M = 6{\cdot}8$; Chapman *et al.* show that the stability of the separated laminar boundary of a two-dimensional flow decreases markedly with a decrease in Mach number at the edge of the separated flow; and therefore it is expected that a pure laminar separation will occur at $R_D = 0{\cdot}12 \times 10^6$.

The average distance of the deflexion region is shown in figure 7 for various Reynolds numbers. For the pure turbulent separation, the separation angle θ_s moderately increases, as observed in the two-dimensional flow. These results are summarized in figure 5, in which the measured data are extrapolated using the most probable inferred values for higher Reynolds numbers, in order to facilitate construction of figure 12 (to be described in §5.1).

On the whole, the general shape and nature of the separated flow over the blunt-spiked hemisphere show a similarity to those of a sharp-spiked hemisphere as obtained by other investigators.

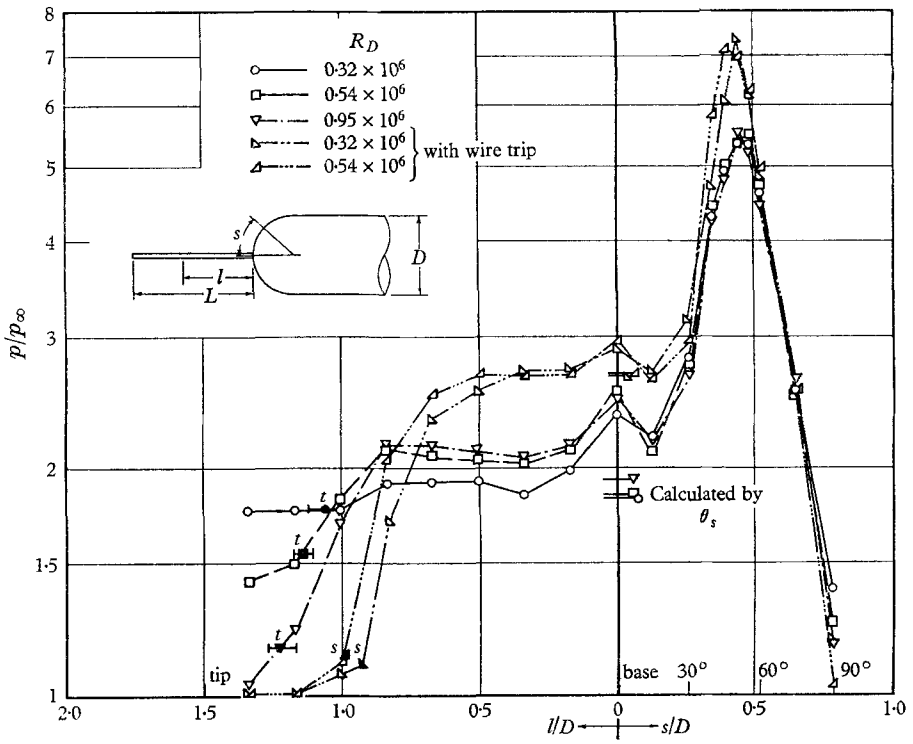

FIGURE 6. Pressure distribution along spike and over body surface for different Reynolds numbers, $L/D = 1{\cdot}5$. Shaded symbols with 't' and 's' denote transition and separation point, respectively.

3.2. *Pressure distribution along spike*

The pressure distribution along the spikes of two different lengths is shown in figures 6 and 7. The pressure rise at the transition is generally very weak for both $L/D = 1{\cdot}5$ and 2 at low Reynolds numbers and becomes stronger as the Reynolds number increases. For $L/D = 2$, the pressure increases gradually in the region between the separation point and the deflexion region of the separated boundary at low Reynolds numbers. For the higher Reynolds numbers with laminar starting of separation, i.e. $0{\cdot}54 \times 10^6$ and $0{\cdot}95 \times 10^6$, the pressure increases rather sharply from the transition (figure 7). This point, i.e. varying degree of pressure increase at the transition, is similar to a two-dimensional separated flow (Chapman *et al.* 1957).

The pressure after the deflexion is nearly constant as is to be expected from the nature of the separated boundary, i.e. formation of a conical shock wave. The pressure calculated using the free-stream Mach number, from the equivalent cone angle θ_s, that replaces the separation region, is shown in figures 6 and 7.

The calculated pressure agrees roughly with the measured values and thus shows that the concept of equivalent constant-pressure cone for the separated region, postulated by Wood (1962), is valid for this case.

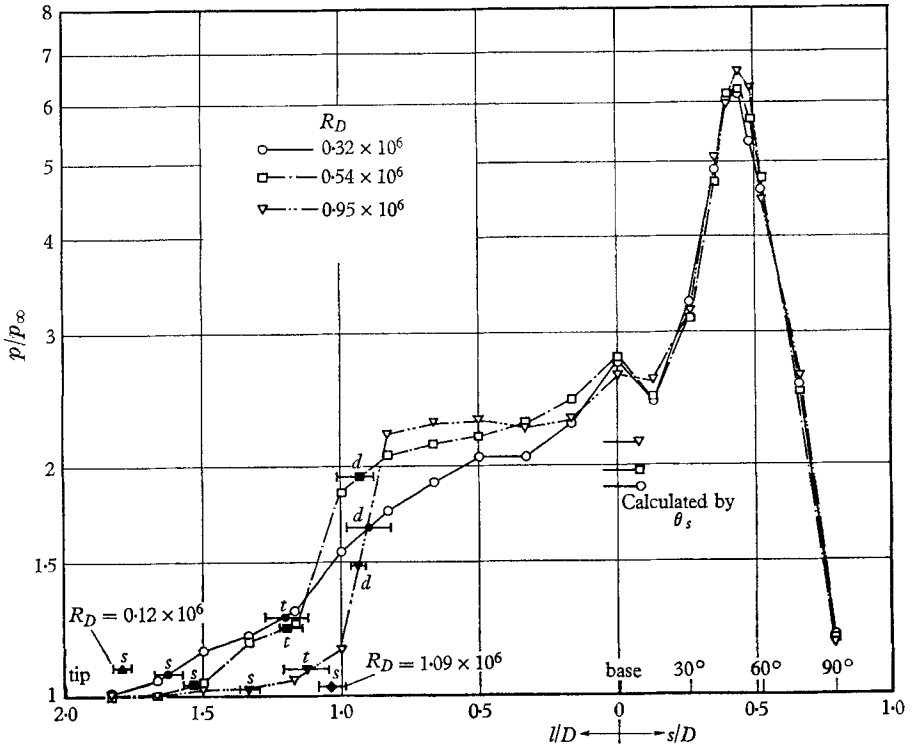

FIGURE 7. Pressure distribution along spike and over body surface for different Reynolds numbers, $L/D = 2$. Shaded symbols with 't', 's' and 'd' denote transition, separation, and deflexion point of separated boundary, respectively.

When a trip is placed at the tip of the spike with $L/D = 1{\cdot}5$, the separation point moves rearward as seen in figure 3 (b). The pressure distribution of this flow with the trip shows a trend similar to a pure turbulent separation of two-dimensional flow over a step (Chapman *et al.* 1957). Thus the effect of perturbing the flow by a trip is seen to be equivalent to increasing the effective Reynolds number. It is seen that the constant pressure reached in the separated region by a spike with a trip is much higher than that reached by a spike without a trip and agrees very closely with the value calculated from the separation angle θ_s.

Comparison of figures 6 and 7 shows that the pressure near the stagnation point is always higher for the longer spike than for the shorter spike. This is in conformity with the fact that the separation angle for the shorter spike is smaller than that for the longer spike. One notices also that the pressure along the spike peaks at the base, i.e. the stagnation point of the body (figures 6 and 7). This agrees with the result for two-dimensional separated flow over a forward-facing step.

3.3 *Pressure distribution over the body surface*

The effect of spike length and Reynolds number on the pressure distribution over the body surface is shown also in figures 6 and 7. The pressure distribution is similar to that over a body with a sharp spike. For all the lengths of spike and test Reynolds numbers, the maximum pressure, i.e. the value at the reattachment point, occurred approximately at 50° from the stagnation point. This maximum pressure is always lower than the stagnation-point value on an unspiked body. The variation of reattachment point due to transition was negligible.

The pressure over the body with a longer spike is always higher than over that with a shorter spike. It can be seen from this result that the pressure drag of a body with a longer spike is greater than that of a body with a shorter spike at this Mach number. Therefore, there must be a critical length of spike which minimizes the pressure drag for a laminar separated flow at a given Reynolds number. The pressure over the body surface was noticeably increased by a boundary layer trip at spike tip as shown. The pressure at reattachment point increases to approximately 35 % above the value obtained without a trip. The reattachment point for the separated flow with a trip is again located at approximately 50° from the stagnation point.

4. Geometry and aerodynamics of injecting orifices

The injecting orifices were drilled normal to the surface and no effort was made to produce an attached flow by contouring the lips. Of the three tested injecting-point locations, the base injection is thought to be least affected by the geometry of the injecting orifice. This is because the base region is already in fully-turbulent motion and the direction of the ejected flow is the same as that of the undisturbed separated-flow motion. The aerodynamics of the injection at the reattachment region will only affect the after-body flow because the turbulence produced here does not affect the upstream flow. The most critical effect of the geometry of injecting orifices on the separated-flow characteristics will be found in the case of spike-tip injection. Since the transition of boundary-layer flow is sensitive to the initial degree of turbulence (Potter & Whitfield 1962), the turbulence of injected air and the injecting-point geometry must be examined for this case.

Examination of the inner radius and the length of the spike-tube and velocity of ejected air, shows that the ejected flow emanating from the spike tip is originally laminar for all the injection rates tested, except for the extremely high rate of injection for which the initial turbulence is not important, i.e. a supersonic injection, described below. The degree of turbulence produced at the spike tip by injection is, therefore, determined by the mechanism of separation and reattachment of the ejected flow at the sharp lip. In the present work, the following three régimes are covered by changing the injection rate.

(i) Laminar subsonic injection. This condition is achieved at the lowest injection rate tested, i.e. $C_{\dot{m}} \simeq 0{\cdot}002$ (see below). Since the Reynolds number R_j, based on the diameter of the spike and ejected-flow velocity, was very small, i.e. less than 10^4, the ejected flow is thought to reattach laminarly on the shoulder of the spike tip. Under this condition the velocity of a laminar boundary layer of

free-stream on the spike surface is increased by the ejected air. The start of laminar separation is seen to move rearward (figure 9(*a*), plate 3) because of this, but the separation is still laminar.

(ii) Turbulent near-sonic injection. This is produced by a near-sonic injection in which ejected air does not expand seriously. Since the Reynolds number of ejected air was moderate, i.e. R_j was between $1{\cdot}5 \times 10^4$ to 3×10^4, the ejected

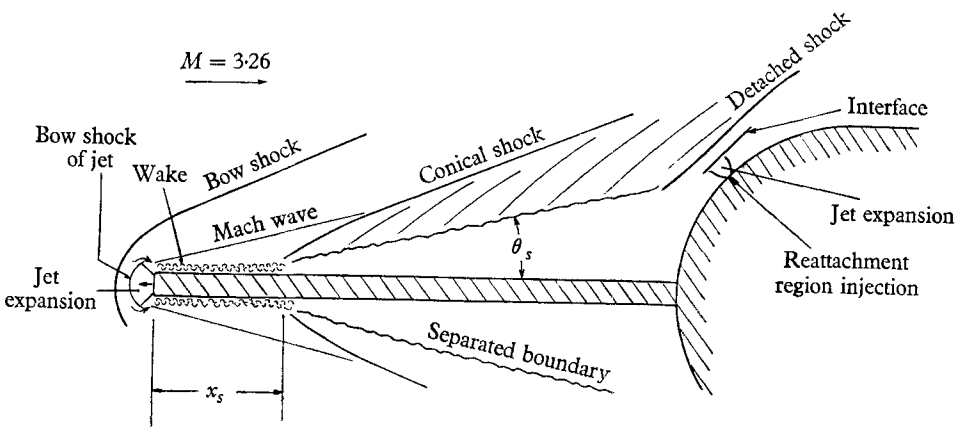

(*a*) Supersonic injection

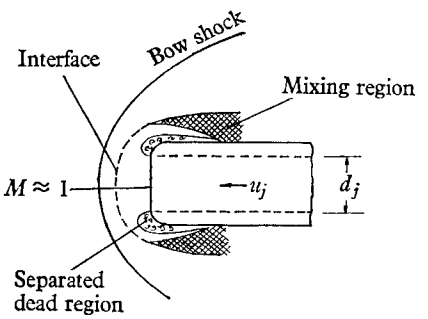

(*b*) Turbulent near-sonic injection

FIGURE 8. Sketch of the observed flow field and detail of the spike-tip flow at high rate of injection.

gas is thought to undergo a turbulent separation. The separation point on the spike is seen to move rearward (figures 8(*a*) and 9(*b*), plate 3). This and the foregoing régime (i) may be the region where the study of Sutton & Finley (1964) pertains.

(iii) Supersonic injection. This condition is produced by a large injection rate. Ejected air is sonic at the lip of spike and expands rapidly through a strong Prandtl–Meyer fan (figure 8(*a*) and 9(*c*), plate 3). The supersonic jet of outcoming flow meets a free-stream and forms an extraneous 'reversed' bow shock wave and subsequently turns around the corner. Under this condition the turning flow

never reattaches on the spike surface, but produces a wake of low pressure. The start of separation over the spike occurs directly from this wake region. At extremely high injection rates a laminar sublayer may evolve underneath the turbulent wake.

The mass injection coefficient, suggested by Warren (1960) can be written for a supersonic injection condition as

$$C_{\dot{m}} = \dot{m}/\rho_\infty U_\infty \pi(\tfrac{1}{2}D)^2 = K\,(p_{0j}/p_0)\,(T_0/T_{0j})^{\frac{1}{2}} A_j,$$

where $\dot{m}$, ρ_∞, U_∞, p_0, T_0 and A_j are mass flow rate, density, velocity, total pressure, total temperature of free-stream and total area of injecting orifices, respectively. The double suffix '$0j$' denotes the stagnation conditions in the injecting air. The constant K depends on free-stream Mach number, model diameter, and discharge coefficient of the orifices, which was calibrated initially.

5. Results for flow with injection

5.1. *Injection from spike tip*

Forward injection of air from the spike tip causes a large variation of separation point at small injection rates for an initially laminar separated flow. For large injection rates, the separation point reaches an almost constant position for all cases. At extremely large injection rates, however, the separation characteristics

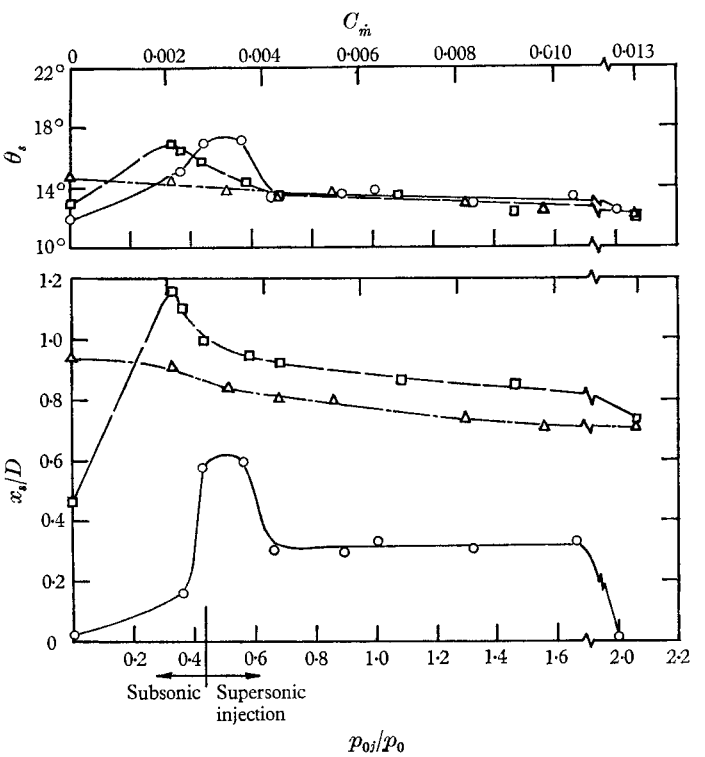

FIGURE 11. Separation point and angle versus different rates of spike-tip injection and injection-pressure ratio. ○, $L/D = 1{\cdot}5$, $R_D = 0{\cdot}54 \times 10^6$; □, $L/D = 2$, $R_D = 0{\cdot}54 \times 10^6$, initially laminar separation; △, $L/D = 2$, $R_D = 1{\cdot}09 \times 10^6$, initially turbulent separation.

approach those of a laminar separated flow (figure 10, plate 4). These results are summarized in figure 11. As seen from figure 11, the maximum rearward shift of laminar separation point for $L/D = 1{\cdot}5$ for initially laminar separated flow occurs at the turbulent near-sonic injection, i.e. injection of type (ii) of §4, corresponding to the injection rate of $C_{\dot{m}} = 0{\cdot}003$. The distance of backward shift at this critical injection rate is extraordinarily large. For $L/D = 2$ and initially-laminar separated flows, the maximum rearward shift of the separation point was observed at the lowest injection-rate tested.

It is seen from these results that the injection from the spike tip critically affects the initial turbulence level. It is thought that a relatively small amount of injection tends to cause a transition of laminar separated flow into a turbulent one. Once the separated flow becomes a turbulent flow, the initial turbulence level has no more effect on the separated flow, and so at high injection rates the separation distance remains almost constant.

A more detailed examination of figure 11 shows that at high injection rates the separation-distance variation does not follow the pattern of the non-injected flow, that is, the separation distance decreases as the injection rate increases, whereas for a non-injected flow the separation distance increases as the Reynolds number increases. The reason for this may be that when a large amount of air is injected from the spike tip, the volume of air emerging into the separated region is increased, thus altering the adverse pressure gradient around the separation point.

It is seen that even when the stagnation pressure of injected air exceeds the free-stream stagnation pressure, the flow is still stable. The local flow around the

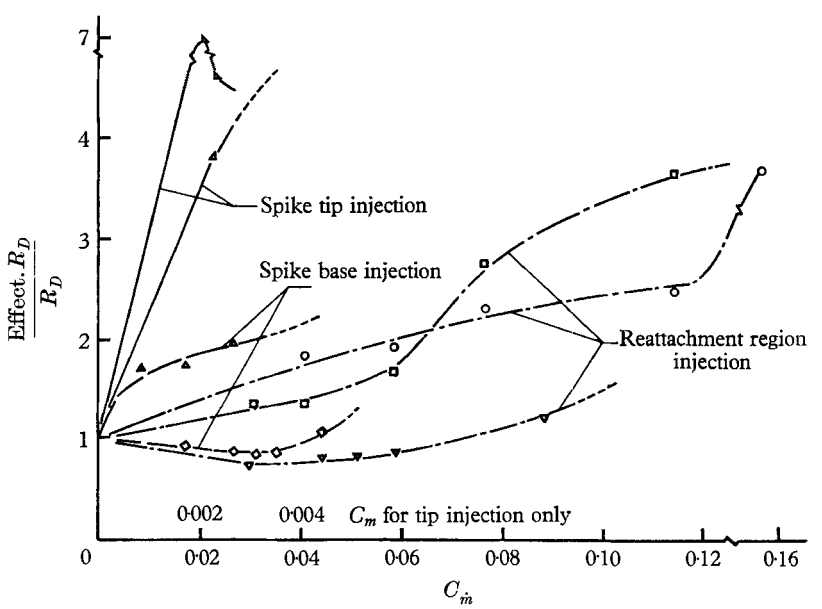

FIGURE 12. Effective Reynolds number *vs.* mass injection rate. ◭, $L/D = 1{\cdot}5$, $R_D = 0{\cdot}54 \times 10^6$; ◺, $L/D = 2$, $R_D = 0{\cdot}54 \times 10^6$; △, $L/D = 2$, $R_D = 0{\cdot}54 \times 10^6$; ◇. $L/D = 2$, $R_D = 1{\cdot}09 \times 10^6$, initially turbulent separation; ○, $L/D = 1{\cdot}5$, $R_D = 0{\cdot}54 \times 10^6$; □, $L/D = 2$, $R_D = 0{\cdot}54 \times 10^6$; ▽, $L/D = 2$, $R_D = 1{\cdot}09 \times 10^6$, initially turbulent separation,

tip including the two bow shocks is stable up to the maximum p_{0j}/p_0 tested, i.e. 4·6. In order to observe the nature of the mixing of the injected air with the free-stream air, water vapour was injected from the spike tip. The result shows that the vapour rapidly freezes and accumulates on the spike base. This observation indicates an emergence of ejected air into the dead region of separation. The location of the reattachment point was not influenced appreciably by the tip injection for the range of injection of the present study.

The dependence of the transition characteristics on the mass-injection rate is shown in figure 12, where the change of effective Reynolds number is plotted against the mass-injection rate. Here the effective Reynolds number was determined from the separation-point location of figure 5 and free-stream conditions.

5.2. *Injection from spike base*

Injection from the base of the spike moves the separation point forward, but does not alter radically the shape of the separated flow up to about $C_{\dot{m}} = 0{\cdot}03$, for which the separation point was shifted to the spike tip (figure 13 (*a*), plate 5). For the injection rate above $C_{\dot{m}} = 0{\cdot}03$ the separated boundary is deformed into

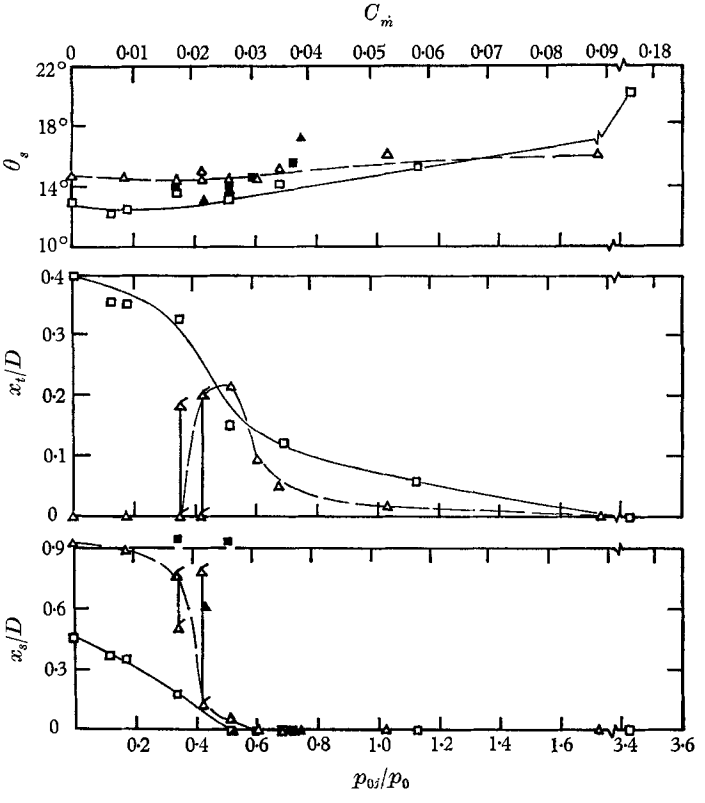

FIGURE 14. Effect of mass injection from spike base and tip upon separation point, transition point and separation angle; supersonic injection, $L/D = 2$. □, Base injection, $R_D = 0{\cdot}54 \times 10^6$; △, base injection, $R_D = 1{\cdot}09 \times 10^6$; ■, base and tip injection, $R_D = 0{\cdot}54 \times 10^6$, tip injection rate is 12·3 % of base injection rate indicated; ▲, base and tip injection, $R_D = 1{\cdot}09 \times 10^6$, same as above.

an ogive shape (figure 13(*b*), plate 5), and is still stable except for the extremely large rate of injection, $C_{\dot{m}} = 0{\cdot}176$. For the spike with $L/D = 2$ at a Reynolds number of $0{\cdot}54 \times 10^6$, the laminar extent of the separated boundary decreases with increase in injection rate as shown in figure 14. For $R_D = 1{\cdot}09 \times 10^6$, for which the separation is initially turbulent, separation becomes a transitional separation and a laminar region appears on injection. For the spike-base injection, the flow condition at the injection orifices was mostly sonic. It was observed that the separation point oscillated back and forth for the injection rate at which a pure turbulent separation changes into laminar separation, i.e. $R_D = 1{\cdot}09 \times 10^6$, as shown in figure 14. The location of the reattachment point remained nearly the same as for that without base injection except at an extremely large rate of injection. The detached distance of the shock at the reattachment point is increased by the injection.

When air is injected from both spike base and tip, the location of the separation point is determined by the relative magnitude of the two injections (see figures 14, 13(*c*), plate 5). That is, if the tip injection is more influential, the separation point moves rearward but moves upstream and even ahead of the spike tip when the base injection is dominant (figure 13(*c*), plate 5). One notices for $L/D = 2$ and $R_D = 1{\cdot}09 \times 10^6$ that a simultaneous injection from tip and base with the ratio 12:100 moves the separation point ahead of the spike tip (figure 14). This shows that the combined injection at the two points is very effective in shifting the separation point forward. These results are again summarized in figure 12, where the effective Reynolds number is determined by the trend of the laminar extent of the separated flow of figure 5.

5.3. *Injection from reattachment region*

The general shape of separated flow is again not altered by the injection from the reattachment region for a value of $C_{\dot{m}}$ of up to 0·585 or $p_{0j}/p_0 = 3{\cdot}43$. For the rate of injection higher than this value, a serious oscillation was observed. The separated flow with the injection from the reattachment region is generally stable independent of the rate of injection. The detached distance of the shock wave at the reattachment point was increased by the injection and an irregular interface of the two flows, i.e. the shear layer of separated boundary and expanding jet of ejected air, appeared as shown in figure 15(*b*) (plate 6) and sketched in figure 8(*a*). For the spike with $L/D = 1{\cdot}5$, the angle of separation is increased and the transition point on the separated boundary is moved upstream by the injection (figure 16). The effect of injection at the reattachment region is similar to that of increasing the step height in a two-dimensional flow over a forward-facing step. It is known for two-dimensional flow that an increase in step height slightly reduces the transition Reynolds number (Chapman *et al.* 1959). Figure 12 shows that the effective Reynolds number generally increases as injection rate increases, except for $L/D = 2$ and $R_D = 1{\cdot}09 \times 10^6$, for which a decrease is observed at low rates of injection.

When air is injected from both spike tip and reattachment region, the effects of two injections are superimposed. The relative magnitude of their influences is shown in figures 15(*c*) (plate 6) and 16.

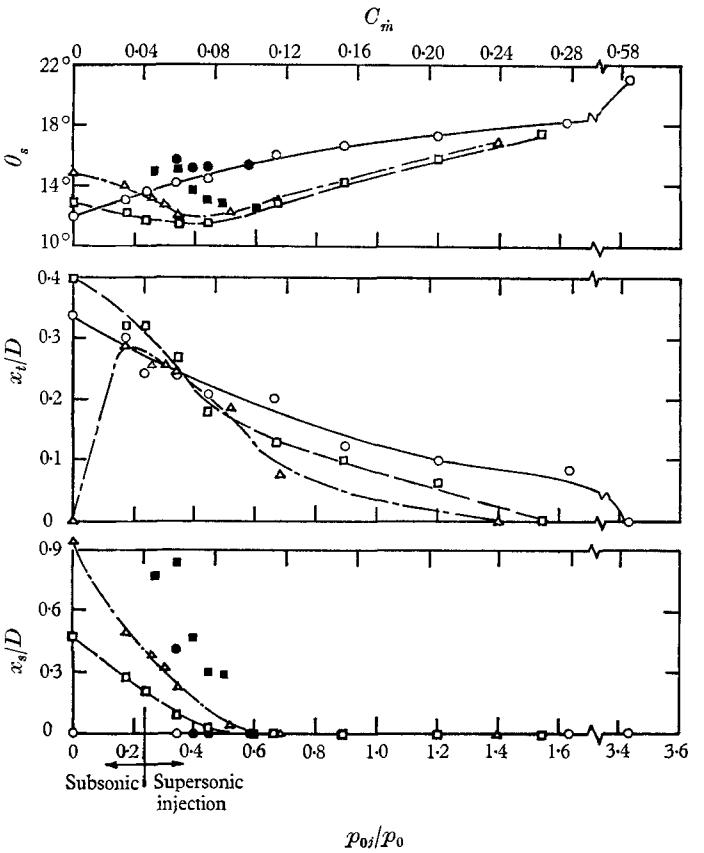

FIGURE 16. Effect of mass injection from reattachment region and spike tip upon separation point, transition point and separation angle. ○, Reattachment-region injection, $L/D = 1{\cdot}5, R_D = 0{\cdot}54 \times 10^6$; □, reattachment-region injection, $L/D = 2$, $R_D = 0{\cdot}54 \times 10^6$; △, reattachment-region injection, $L/D = 2, R_D = 1{\cdot}09 \times 10^6$; ●, reattachment-region and spike-tip injection, $L/D = 1{\cdot}5$, $R_D = 0{\cdot}54 \times 10^6$, spike-tip injection rate is 3·7% of reattachment-region injection rate indicated; ■, reattachment and spike-tip injection, $L/D = 2$, $R_D = 0{\cdot}54 \times 10^6$, same as above.

6. Discussion

The immediate effect of mass injection at the spike tip may be divided into (i) disturbing perturbation, and (ii) mass-flow-rate increase, i.e. displacement effect. For the second effect, the present investigation shows that the increase in mass flow-rate appears as an increase in volume of the dead region of the separation, i.e. forward shifting of the separation point. For the first effect, an effort has been made to minimize the turbulence level by keeping the local Reynolds number of ejection sufficiently small. The results show that, at least for $L/D = 1{\cdot}5$, a relatively turbulence-free injection is achieved at $C_{\dot{m}} = 0{\cdot}002$ (figure 11). Even at this turbulence-free injection, however, the effective Reynolds number is seen to increase by a factor of nearly 4. The possible explanation of the destabilizing effect of tip injection may be that, due to the difference in temperature, and hence density, between the free-stream and ejected flow, the mixing of

the two gases more easily evolves into a turbulent motion than an ordinary boundary-layer flow. Thus it is doubtful whether one can prevent this destabilizing effect by adopting the technique of attached potential flow (Eminton 1960; Tucker 1963 and Hall 1963) for a transitional separated flow. Even when the ejecting lip is shaped according to the potential-flow theory so as not to cause a separation a turbulent motion may originate from the interface of two gases unless a due precaution is taken. Further investigations into the problem of decreasing the turbulence level of mixing flow is desirable.

Of the three injecting-point locations tested, the base and reattachment-region injection appear as slightly stabilizing at low injection rates if the separation is initially turbulent. Thus the intuitive effort of Wood (1962) seems to be in the right direction under this condition. As for the total heat transfer to the body, however, the reattachment-region injection or combined injection from spike tip and base appear to be as potentially effective in heat protection as the base injection. The result of the present work can be used to estimate the possible range of injection rates for a stable flow-configuration for heat-transfer-rate measurement. The measurement of heat-transfer rate in the presence of injection is currently being undertaken at Seoul National University under the conditions reported in the present paper.

7. Conclusions

This investigation shows that the pressure distribution along the spike in the transitional Reynolds-number régime is similar to that in a two-dimensional separated flow, except that the separated boundary deflects behind the transition region. For a transitional separation, the pressure over the surface is higher for a longer spike than that for a shorter spike. The pressure on the body surface is increased considerably when initially laminar separated flow becomes turbulent on perturbing the flow by a trip at the spike tip.

The investigation of injection effects on separated flow shows that the aerodynamics of injection from a spike tip affects the separated flow seriously. The general stability of separated flow is unaffected by the injection from the spike tip or base or reattachment region, even for a fairly high rate of mass injection. Injection from the reattachment region increases the effective Reynolds number for a large rate of injection. The effect of spike-tip injection is similar to that of perturbing the flow by a trip, and is to increase the effective Reynolds number by a large factor when the flow is initially in the laminar separated régime. A turbulence-free tip injection can be achieved only for $L/D = 1{\cdot}5$ at $C_{\dot{m}} = 0{\cdot}002$. Injections from the spike base and the reattachment region generally increase the effective Reynolds number, but tend slightly to stabilize the separated flow if the initial separated flow is in a purely turbulent régime.

REFERENCES

BOGDONOFF, S. M. & VAS, E. I. 1959 *J. Aero. Sci.* **26**, 65.
BRADFIELD, W. S. & SHEPARD, J. J. 1959 *Aero Space Engng* **18**, 37.
CHAPMAN, D. R., KUEHN, D. M. & LARSON, H. K. 1957 *NACA TN* no. 3869.
CRAWFORD, D. H. 1959 *NASA TN* no. D-118.
EMINTON, E. 1960 *R.A.E. TN Aero* no. 2711.
HAHN, M. 1964*a* *J. Korean Mech. Soc.* **4**, 35.
HAHN, M. 1964*b* *J. Nuclear Soc.* (*Korea*), **4**, 83.
HALL, M. G. 1963 *R.A.E. TN Aero* no. 2910.
POTTER, J. L. & WHITFIELD, J. D. 1962 *J. Fluid Mech.* **12**, 501.
STALDER, J. R. & NIELSEN, H. V. 1954 *NACA TN* no. 3287.
SUTTON, E. P. & FINLEY, P. J. 1964 *Arch. Mech. Stosowanej* (Poland), p. 781.
TUCKER, L. M. 1963 *R.A.E. TN Aero* no. 2923.
WARREN, C. H. E. 1960 *J. Fluid Mech.* **8**, 400.
WOOD, C. J. 1962 *J. Fluid Mech.* **12**, 614.

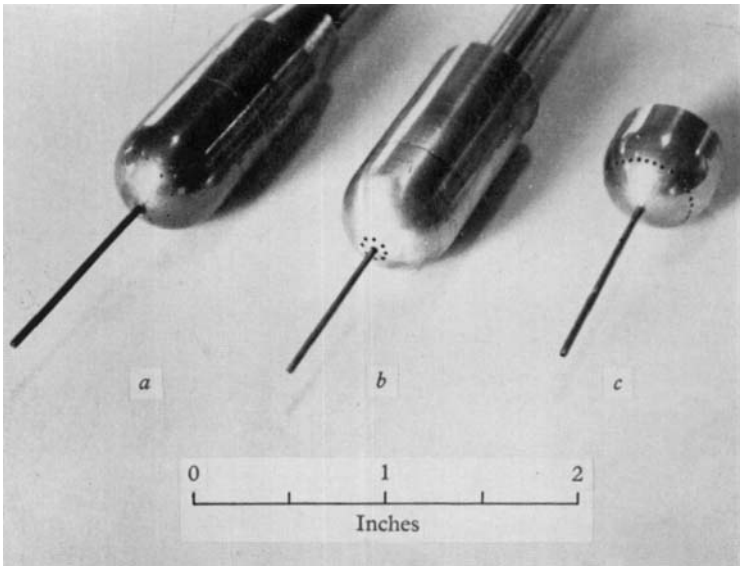

FIGURE 1. Photograph of models: (*a*) Pressure model, orifices at 15, 30, 40, 45, 50, 55, 60, 75 and 90° from stagnation point. (*b*) Spike-base injection model. (*c*) Reattachment-region injection model.

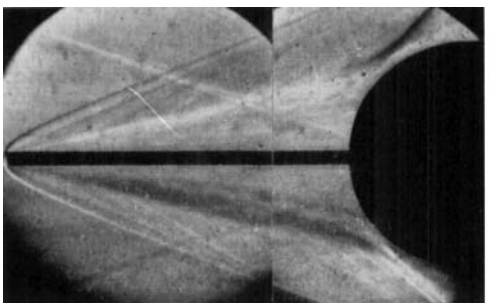

(*a*) Plain spike, $L/D = 1{\cdot}5$, $R_D = 0{\cdot}54 \times 10^6$.

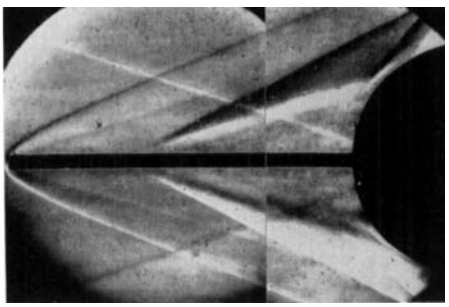

(*b*) Tripped with wire near tip, $L/D = 1{\cdot}5$, $R_D = 0{\cdot}54 \times 10^6$.

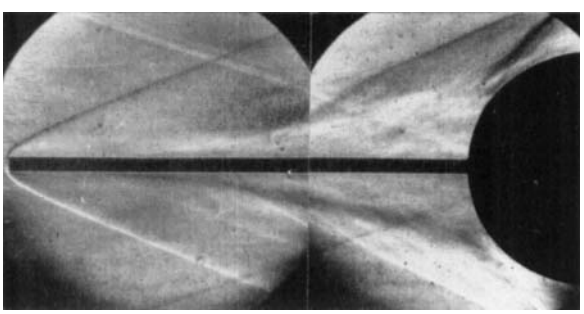

(*c*) Plain spike, $L/D = 2$, $R_D = 0{\cdot}54 \times 10^6$.

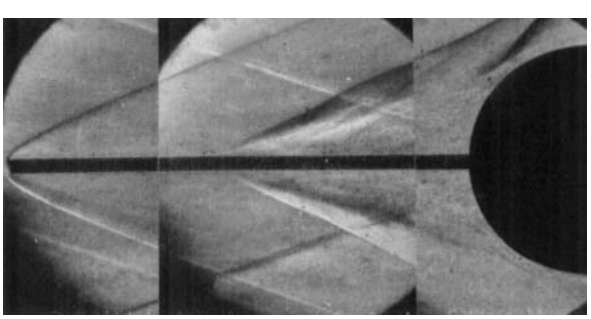

(*d*) Plain spike, $L/D = 2$, $R_D = 1{\cdot}09 \times 10^6$.

FIGURE 3. Typical schlieren photographs of flow without injection.

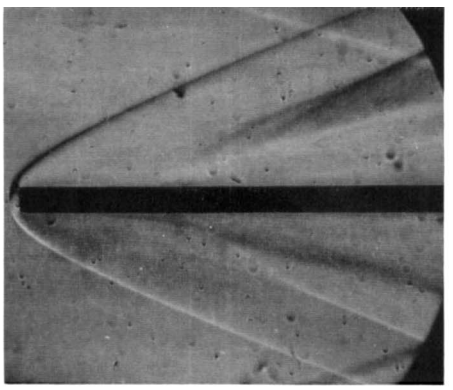

(*a*) Laminar subsonic injection, $C_{\dot{m}} = 0{\cdot}002$, $p_{0j}/p_0 = 0{\cdot}366$.

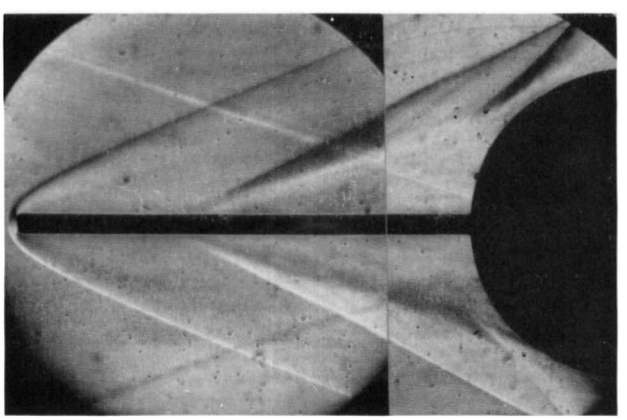

(*b*) Turbulent near-sonic injection, $C_{\dot{m}} = 0{\cdot}003$, $p_{0j}/p_0 = 0{\cdot}432$.

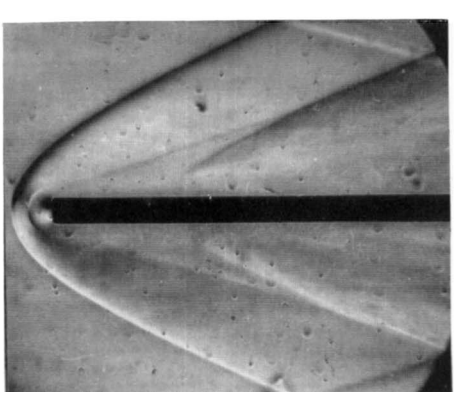

(*c*) Supersonic injection, $C_{\dot{m}} = 0{\cdot}01$, $p_{0j}/p_0 = 1{\cdot}66$.

FIGURE 9. Typical schlieren photographs of flow field around the spike tip with injection, $L/D = 1{\cdot}5$, $R_D = 0{\cdot}54 \times 10^6$.

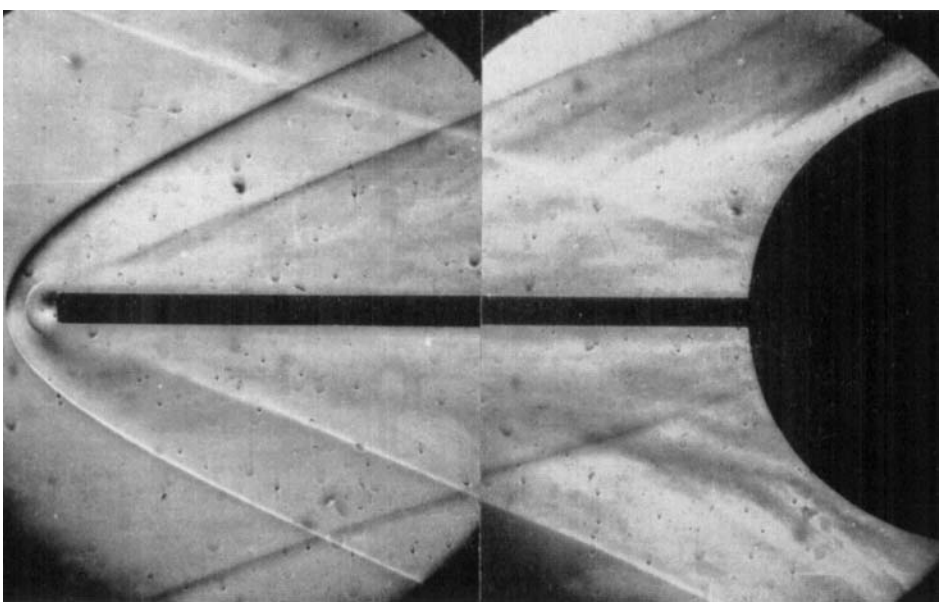

FIGURE 10. Typical schlieren photograph of spike tip with large rate of injection, $C_{\dot{m}} = 0{\cdot}013$, $p_{0j}/p_0 = 2{\cdot}0$, $L/D = 1{\cdot}5$, $R_D = 0{\cdot}54 \times 10^6$.

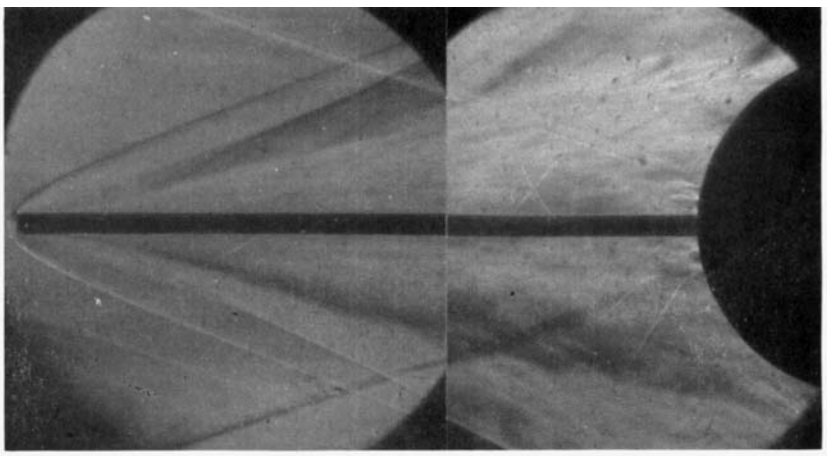

(*a*) C = 0·027 from base, p_{0j}/p_0 = 0·519.

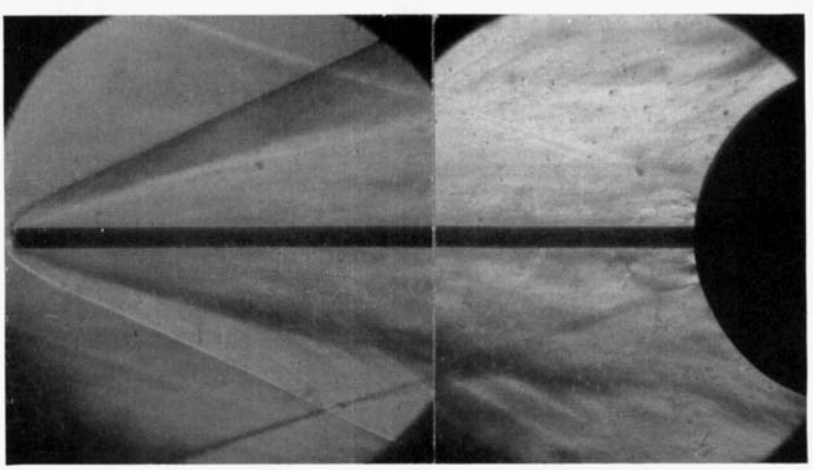

(*b*) $C_{\dot{m}}$ = 0·035 from base, p_{0j}/p_0 = 0·682.

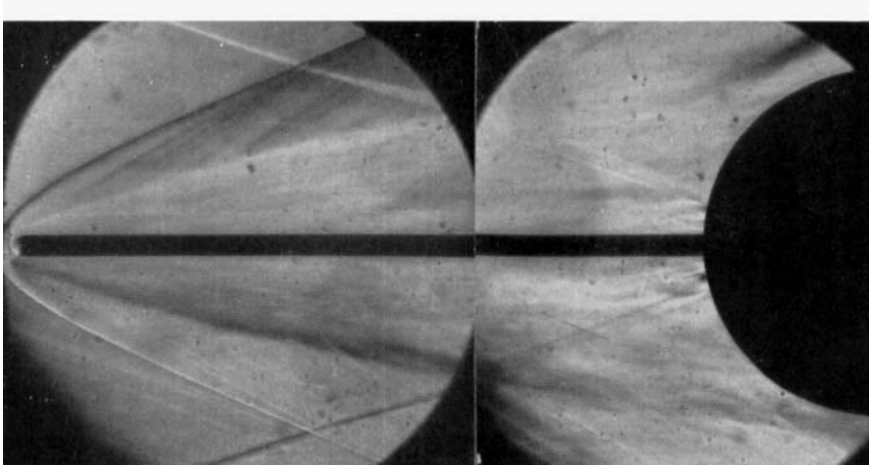

(*c*) $C_{\dot{m}}$ = 0·027 from base, $C_{\dot{m}}$ = 0·003 from tip, p_{0j}/p_j = 0·519.

FIGURE 13. Typical schlieren photographs of flow with spike tip and base injections, L/D = 2, R_D = 1·09 × 10^6.

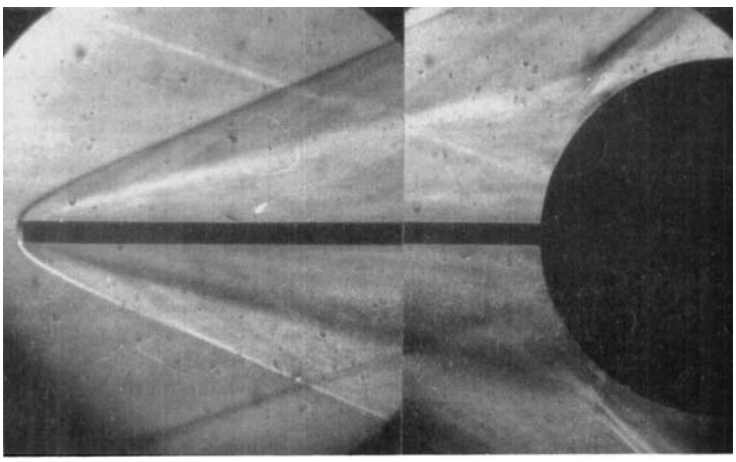

(*a*) $C_{\dot{m}} = 0{\cdot}041$ from reattachment region, $p_{0j}/p_0 = 0{\cdot}24$.

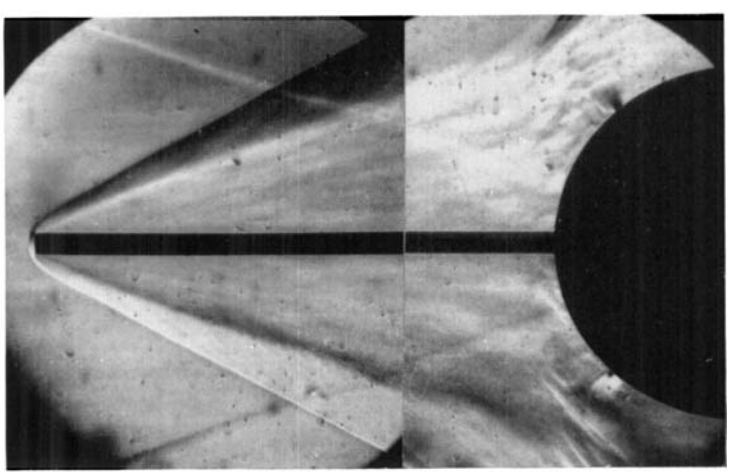

(*b*) $C_{\dot{m}} = 0{\cdot}278$ from reattachment region, $p_{0j}/p_0 = 1{\cdot}63$.

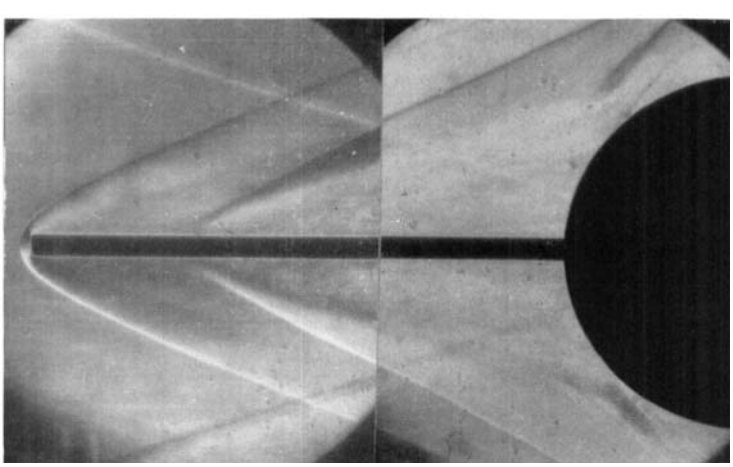

(*c*) $C_{\dot{m}} = 0{\cdot}059$ from reattachment region, $C_{\dot{m}} = 0{\cdot}002$ from spike tip, $p_{0j}/p_0 = 0{\cdot}35$.

FIGURE 15. Typical schlieren photographs of flow with injection from reattachment region and spike tip, $L/D = 1{\cdot}5$, $R_D = 0{\cdot}54 \times 10^6$.